Ann. Occup. Hyg., Vol. 55, No. 9, pp. 1016–1036, 2011
Published by Oxford University Press
on behalf of the British Occupational Hygiene Society
doi:10.1093/annhyg/mer073

Exposure and Emissions Monitoring during Carbon Nanofiber Production—Part I: Elemental Carbon and Iron–Soot Aerosols

M. EILEEN BIRCH*, BON-KI KU, DOUGLAS E. EVANS and TONI A. RUDA-EBERENZ

Division of Applied Research and Technology, National Institute for Occupational Safety and Health, 4676 Columbia Parkway, MS-R5, Cincinnati, OH 45226, USA

Received 15 April 2011; in final form 15 July 2011; published online 28 September 2011

Production of carbon nanofibers and nanotubes (CNFs/CNTs) and their composite products is increasing globally. High volume production may increase the exposure risks for workers who handle these materials. Though health effects data for CNFs/CNTs are limited, some studies raise serious health concerns. Given the uncertainty about their potential hazards, there is an immediate need for toxicity data and field studies to assess exposure to CNFs/CNTs. An extensive study was conducted at a facility that manufactures and processes CNFs. Filter, sorbent, cascade impactor, bulk, and microscopy samples, combined with direct-reading instruments, provided complementary information on air contaminants. Samples were analyzed for organic carbon (OC) and elemental carbon (EC), metals, and polycyclic aromatic hydrocarbons (PAHs), with EC as a measure of CNFs. Transmission electron microscopy with energy-dispersive X-ray spectroscopy also was applied. Fine/ultrafine iron-rich soot, PAHs, and carbon monoxide were production byproducts. Direct-reading instrument results were reported previously [Evans DE *et al.* (Aerosol monitoring during carbon nanofiber production: mobile direct-reading sampling. *Ann Occup Hyg* 2010;54:514–31.)] Results for time-integrated samples are reported as companion papers in this Issue. OC and EC, metals, and microscopy results are reported here, in Part I, while results for PAHs are reported in Part II [Birch ME. (Exposure and Emissions Monitoring during Carbon Nanofiber Production—Part II: Polycyclic Aromatic Hydrocarbons. Ann. Occup. Hyg 2011; 55: 1037–47.)]. Respirable EC area concentrations inside the facility were about 6–68 times higher than outdoors, while personal breathing zone samples were up to 170 times higher.

Keywords: carbon nanofiber; elemental carbon; nanomaterial; nanotube; occupational exposure; ultrafine

INTRODUCTION

Nanotechnologies are expected to have broad impact on many sectors of the US economy. Some estimates project that growth in this sector will require up to 2 million workers globally by 2015 (Roco and Bainbridge, 2005). Nanotechnologies have immense promise, but there are multiple impediments, technical and other, that must be overcome before this promise can be realized (BCC Research, 2010). The challenges and differing opinions regarding commercial applications are apparent in the widely different estimates of nanotechnology markets (BCC Research, 2010). Estimates for 2010 ranged from ~$15.7 billion to $1 trillion. Estimates for 2015 are even more disparate. One estimate projects a market worth over 2.4 trillion dollars by 2015 (BCC Research, 2010), corresponding to a compound annual growth rate of 11.1%. Another projects a value up to $4 trillion in 'manufactured goods', a compound annual growth rate of 41% (Lux Research, 2008). These large differences reflect different analysis methods, assumptions, and market

*Author to whom correspondence should be addressed.
Tel: +1-513-841-4298; fax: +1-513-841-4545;
e-mail: mib2@cdc.gov

definitions. According to a recent report, worldwide sales revenues for nanotechnologies were $11.67 billion in 2009, with a predicted increase to more than $26 billion by 2015 (BCC Research, 2010). This latter estimate for 2015 is far different than the oft-cited trillion-dollar figure but may be more realistic. It includes nanotechnology products (nanomaterials, 'nanotools', and 'nanodevices') rather than all 'nanotechnology-enabled' products. In 2009, the largest nanotechnology product segments were nanomaterials, with an estimated worth of $9 billion and a projected increase to about $19.6 billion in 2015 (BCC Research, 2010).

Carbon nanofibers and nanotubes (CNFs/CNTs) are an important class of nanomaterials with many potential applications. Production of CNFs/CNTs and composite products is increasing globally, and manufacturing processes are rapidly changing to produce new materials with advanced properties. For commercial applications, useful properties of CNTs include high tensile strength, high aspect ratios (1:1000 or more), and unique electrical, magnetic and optical characteristics. Applications include electronics, flat panel displays, batteries and fuel cells, thermoplastic additives (to impart conductivity), and biomedical science. CNFs exhibit properties between those of CNT and carbon fibers. At relatively low loadings (e.g. 1–8% by weight), CNFs are being used to improve the thermal, electrical, and mechanical properties of a wide variety of polymer-based composite materials. Applications include high-performance products such as coatings and composites for aerospace, automobiles, sports equipment, and construction. In 2004, an annual global production of CNFs and CNTs was reported as 65 tons per year (Cientifica, 2005). In 2007, the global capacity for multiwalled carbon nanotube (MWCNT) production was reported to be ~300 tons per year (WTEC, 2007). By 2011, it is forecasted that CNTs will constitute a $460 million market (Holman *et al.*, 2007).

CNFs/CNTs vary greatly in their chemical and physical properties, including particle shape, size, and structure; surface area, functionalization, reactivity, and charge; metal content; and aggregation state. CNFs can have stacked cupped, stacked graphene, or hollow-tube structures that are similar to MWCNTs in several respects. Namely, their diameters are similar, with typical CNF diameters being in the 50–200 nm range (Ku *et al.*, 2006) and MWCNTs having diameters up to 100 nm (Wang *et al.*, 2006); structures in both materials are tubular, with hollow cores; and the tubes/fibers in both materials usually are bundled/entangled, though discrete tubes/fibers can be found (Ku *et al.*, 2006; Wang *et al.*, 2007). In contrast, single-walled carbon nanotubes (SWCNTs) have much smaller diameters, typically 1–10 nm, and they tend to form highly entangled structures with a nest-like appearance and consisting of bundles of fibers or 'ropes' (Shvedova *et al.*, 2005; Maynard *et al.*, 2007). According to an International Organization for Standardization (ISO) definition, the primary characteristic that distinguishes CNFs from CNTs is alignment of the graphene plane. If the plane and fiber axis are not parallel, the structure is defined as a CNF. If the alignment is parallel, the structure is considered a CNT (ISO/TS 27687:2008, 2008). In practice, commercially produced CNFs contain, along with stacked cup and other structures, hollow-tube structures (e.g. see Fig. 7) having lengths that run from tens of micrometers to several centimeters, with average aspect ratios >100.

High volume production of CNFs/CNTs may be an exposure risk for workers, especially manual handling in open areas. These materials may be harmful when inhaled because of their size, persistence, composition, and structure. Inflammation, rapid onset pulmonary fibrosis, granulomas, oxidative stress, and mutagenicity have been observed in inhalation studies of mice exposed to SWCNTs (Shvedova *et al.*, 2005, 2008). Dermal inflammation also has been reported (Murray *et al.*, 2009). More alarming is the prospect of asbestos-like pathology, as reported for MWCNTs injected into the abdominal cavities of mice (Poland *et al.*, 2008). A similar study of CNFs has not been conducted, but acute inflammation and early onset of pulmonary fibrosis were observed in mice exposed to CNFs by pharyngeal aspiration (Kisin *et al.*, 2010). A review of the current toxicological literature and draft risk assessment on CNFs/CNTs was recently released by the National Institute for Occupational Safety and Health (NIOSH, 2010) for public comment. A single recommended exposure level was proposed (7 $\mu g\ m^{-3}$); however, it is recognized that the diverse properties of these materials may impart a range of toxicities. As an example, in a recent comparison of inflammatory responses to different types of CNTs administered to the peritoneum of mice, long thick MWCNTs caused DNA damage and severe inflammatory effects, while similar SWCNTs caused little effect, and short thin MWCNTs had no effect (Yamashita *et al.*, 2010). These findings suggest important differences in the biological responses of CNFs/CNTs.

CNFs/CNTs have been produced for some years now, yet relatively few studies at facilities that produce/use these materials commercially have been reported (Maynard *et al.*, 2004; Methner *et al.*, 2007; Evans *et al.*, 2010; Lee *et al.*, 2010), and personal

exposures were not monitored. Given the potential health hazards, there is an immediate need for toxicity and exposure data on CNFs/CNTs, with inhalation being the primary concern. An extensive study was conducted at a facility that manufactures and processes CNFs. Filter, sorbent, cascade impactor, microscopy, and bulk samples, combined with direct-reading instruments, provided complementary information regarding the composition, source, and concentrations of air contaminants. Samples were analyzed for organic carbon (OC) and elemental carbon (EC), metals, and polycyclic aromatic hydrocarbons (PAHs), with EC as a measure of CNFs. Transmission electron microscopy with energy-dispersive X-ray spectroscopy (TEM/EDS) also was applied. Direct-reading monitoring results were reported previously (Evans *et al.*, 2010). Findings for time-integrated samples are reported as companion papers in this Issue. In addition to CNFs, fine/ultrafine iron-soot aerosol, PAHs, and carbon monoxide were found as production byproducts. OC and EC, metals, and microscopy results are reported herein, while results for PAHs are reported separately (Birch, 2011).

FIELD SURVEYS

Facility and process description

Surveys were conducted at a facility that manufactures and processes vapor-grown CNFs. At the time of the surveys, the annual CNF production was ~31 000 pounds, and two different reactors, hereafter referred to as 'A' and 'B', were operating. Raw CNF products were discharged from the reactors through extruders. At reactor A, a compressed raw product was manually pulled from an open trough into which the product was extruded. The raw material was collected at ~30-min intervals, but the number of batches collected and time between collections varied. The product was broken into smaller pieces and placed in an open box lined with a large plastic bag. A second newer reactor (B) produced small CNF clumps as the product was extruded directly into a collection box. Both reactors operated under positive pressure and CNF collection was done in the open workplace. After collection, the plastic bag was closed and the raw CNFs were taken to the processing area for debulking and purification.

The raw CNF products were processed in multiple steps to obtain the final product. First, they were loaded into a hopper/mixer where they were mixed with an aqueous solution. Any remaining large clumps of compressed product from reactor A were manually broken into smaller pieces prior to loading the hopper. After mixing with the solution, the resulting CNF cake was placed in a ventilated oven to dry. When dry, the batch was discharged into a drum containing a plastic bag. The bag of CNF material was poured into another hopper feeding a thermal treatment system for removal of organic and metal impurities. The material was automatically conveyed through the system and the final product was discharged (openly) into a plastic bag inside a box. About 15 pounds of product was collected before the bag was manually removed, closed, and replaced.

The CNF facility has an open-floor plan with ~22 000 square feet of floor space and ceilings ~18 feet high. Synthesis and processing operations were performed in different areas but these areas were not separated. A separate room with a large window to the plant was used as a control room. A small interlock area separated the plant from the control room, and from the administrative areas, but the interlock was not operating during the surveys. The administrative areas included several offices, a conference room, and a small kitchen. Facility and plant operations are described in detail elsewhere (Evans *et al.*, 2010).

Products

The CNF product is formed in the gas phase as an entangled mass. Based on the manufacturer's specifications, it is a high purity material that is 99.9% fibrous and has very low metal content. It is described as a highly graphitic, low-cost tubular material having walls composed of angled graphite sheets, and with physical properties similar to graphite. The fibers have an outer chemically vapor deposited (CVD) layer of carbon and an inner tubular (with hollow core) graphitic layer beneath the CVD layer. The fiber structure, called 'stacked cup' or 'herringbone', has exposed edge planes along the entire surface. The edge sites are highly reactive and allow chemical modification for maximum mechanical reinforcement in polymer composites. Fiber diameters range from 70 to 200 nm, significantly larger than SWCNTs (e.g. 1–3 nm). The average diameter of the product produced during the surveys was reported to be ~150 nm. The lengths of the as-produced fibers are estimated to be from 50 to 200 μm. Different fiber grades are available and depend on the type of thermal treatment received.

Air monitoring

Air monitoring was conducted over a total of 4 days: two consecutive days in December and on 1 day each during the first and second weeks of

February. Five locations inside the facility were monitored: (i) the control room, (ii) the CNF reactor (synthesis) area, (iii) the CNF processing areas, (iv) a maintenance area, and (v) a conference room in an office area. Personal breathing zone samples were collected for employees working mainly in the reactor and thermal treatment areas. Air samples were collected in a conference room to evaluate possible contamination of the administrative areas. Samples also were collected outdoors as a measure of environmental background.

METHODS

Specific surface area

Measurement of Brunauer, Emmett, and Teller (BET) specific surface area (SSA) was performed with a Micromeritics Gemini 2375 Surface Area Analyzer. Bulk CNF samples were degassed in high purity nitrogen for 30 min at 90°C and then 90 min at 200°C. The SSAs were determined by a five-point BET measurement with ultra high purity nitrogen as the adsorbate. The following relative pressures (P/Po, where P is pressure of adsorbate gas and Po is its saturation pressure) used were 0.05, 0.10, 0.15, 0.2, and 0.25. The precision of the method was reported as 5%.

Microscopy samples

Sioutas cascade impactors (Cat. No. 225-370; SKC Inc., Eighty Four, PA, USA) were used to collect size-classified aerosol for TEM analysis. The impactor is a personal sampling device with four impaction stages (A, B, C, and D) and an after filter. It classifies particles into five size ranges according to aerodynamic diameter: <0.25 μm (after filter), 0.25–0.50 μm (Stage D), 0.5–1.0 μm (Stage C), 1.0–2.5 μm (Stage B), and 2.5–10 μm (Stage A). The impactor was operated at a flow rate of 9 l min^{-1} using an attached battery-powered pump (Leland Legacy, Cat. No. 100-3000; SKC Inc.,).

Two TEM grids, a lacey carbon-coated nickel grid and a continuous silicon monoxide-coated nickel grid (both 400 mesh), were placed on the impactor stages to collect the aerosol fractions. To secure the grids, properly sized sections were cut from the adhesive area of 3M Post-it® Notes and used on each of the four stages as impaction substrates. The adhesive portion faced upward and secured the grids in place. The grids were easily removed for TEM analysis without damage. A 37-mm, 2.0-μm PTFE filter (SKC Inc.) was used as the after filter.

Prior to the field surveys, the Sioutas impactors were assembled as described and tested in the laboratory. CNF material obtained from the facility where the surveys were conducted was aerosolized by agitation in a vortex shaker (Ku *et al.*, 2006) for several minutes. The CNF aerosol was fed to a sampling manifold and collected by the impactors. TEM analyses of the grids indicated that particle bounce or resuspension may have occurred when the stages were not coated with oil, as reported for a study of SWCNTs (Baron *et al.*, 2008). To minimize particle bounce on all stages, we followed the approach used by Baron *et al.* (2008). Specifically, a pair of Sioutas impactors was prepared for sampling at a given location. Oiled (oleic acid) 25-mm mixed cellulose ester (MCE) filters (SKC Inc.) were used on every other stage of each impactor. One of the impactors was loaded with oiled filters on Stages A and C, while Stages B and D were uncoated and used to sample particles onto the TEM grids. The second impactor contained oiled filters on Stages B and D, while Stages A and C were used for particle sampling onto TEM grids. This approach provided TEM data for all four stages (plus after filter) and minimized bounce to the adjacent lower stage.

Three pairs of impactors (six total) with oiled substrates on alternate stages were prepared for field sampling. A pair was operated in the reactor area, the thermal treatment (processing) area, and in a maintenance area. Precalibrated pumps were used to draw air through the samplers for ∼5 to 20 min, depending on the particle concentration. An impactor-based electrostatic precipitator (ESP) (Ku and Maynard, 2005) also was used to collect polydisperse particles in these same three areas and in the dryer (processing) area.

The morphology and size of the particles collected on the TEM grids in the impactors were characterized by a Philips CM 20 TEM. The elemental composition of the particles was determined by EDS (EDAX Inc.). Spectra were recorded at an operating voltage of 200 keV using GENESIS software (EDAX). The resolution of the detector is 133.5 eV.

In addition to the air samples, bulk samples of CNFs were examined. A small amount of powder was placed in a 1.5-ml vial containing ∼1.0 ml of isopropyl alcohol and the mixture was sonicated for at least 5 min (some samples required 10–15 min for dispersion). A drop of the resulting suspension was applied to a lacey carbon-coated TEM grid (200 mesh copper; SPI) and allowed to dry. Samples were analyzed on a JEOL JEM-3010 TEM operated at 300 kV. Images were recorded by a Gatan Ultrascan high resolution CCD camera operated with Digital Micrograph software (Gatan). An Oxford INCA EDS system was used for elemental analysis.

Representative images and spectra were acquired from at least three areas of the sample.

Bulk samples also were examined by scanning electron microscopy (SEM). Samples were dispersed on beryllium substrates (using amyl acetate and a tungsten needle) and were examined on a JEOL JSM-6480LX SEM using a working distance of 10 mm and accelerating voltage of 10 kV for imaging and 30 kV for EDS (Oxford INCA EDS system). Images were acquired from three representative areas at a magnification of ×1500.

OC and EC samples

Standard, three-piece 37-mm plastic cassettes (SKC Inc.) loaded with tandem quartz-fiber filters (Tissuequartz™ 2500 QAT-UP; Pall Corp., Ann Arbor, MI, USA) were used to collect air samples for OC–EC analysis. The cassettes were operated at 7 l min^{-1} in an open-face configuration. Alongside the open-face cassettes, cyclone samplers (GK2.69; BGI Inc., Waltham, MA, USA) fitted with the three-piece cassettes were operated at 4.3 and 1.6 l min^{-1} to collect respirable and/or thoracic dust, respectively. Leland Legacy pumps (SKC Cat. No. 100-3000) were used with the open-face cassettes, while PCXR8 pumps (SKC Cat. No. 224-PCXR8) were used with the cyclones.

In addition to the open-face 37-mm cassettes and cyclones, a Micro-Orifice Uniform-Deposit Impactor (MOUDI™ 110; MSP Corp., Shoreview, MN, USA) and Sioutas cascade impactors (SKC Cat. No. 225-370) were used to collect size-classified aerosol for OC–EC (and metals) analysis. As done with the Sioutas impactor pairs used to collect TEM samples, a filter soaked with oleic acid was placed on every other stage of the Sioutas impactors. However, for OC–EC analysis, 25-mm quartz-fiber filters were used on alternate stages (instead of TEM grids), and a 37-mm quartz filter was used as an after filter rather than PTFE. The impactors were operated at the same three locations noted previously.

The 110 MOUDI has an inlet stage that collects particles >10 μm and 10 impaction stages with nominal cut points of 10 μm (Stage 1), 5.6, 3.2, 1.8, 1.0, 0.56, 0.32, 0.18, 0.1, and 0.056 μm (Stage 10). Forty-seven millimeters quartz-fiber filters were used on Stages 1, 3, and 5, and a 37-mm quartz-fiber filter was used as the after filter. Oil-soaked MCE filters were used on the other stages. Before use, the quartz filters were flattened to ∼0.11 mm by gently rolling a clean metal cylinder over them. The number of quartz filters used was limited by the high pressure drop that occurred when they were placed on the lower stages of the MOUDI. For this reason, the flattened quartz filters could only be used on the upper stages specified. The flow rate for the MOUDI was calibrated to 30 l min^{-1} with a mass flow meter (Model 3063; TSI Inc., Shoreview, MN, USA). The MOUDI was operated in the thermal treatment and reactor areas of the facility.

All quartz filters and impaction substrates were analyzed for OC and EC by NIOSH Method 5040 (Birch, 2004; NIOSH, 2003). Bottom filters in the 37-mm cassettes with tandem quartz filters were analyzed and results were used to correct the sample filter (top) results for adsorbed organic vapor, thereby giving a better measure of particulate OC (Birch, 2004; Noll and Birch, 2008). Multiple analyses were required for the impactor substrates because the sample was deposited in spots or lines over a substrate rather than evenly across the filter (as with 37- or 25-mm filters). In such cases, the entire sample must be analyzed because a single punch, normally 1.5cm^2, from the substrate is not representative of the entire deposit. For some samples, multiple punches from a substrate were analyzed together to reduce the number of analyses required. Manual OC–EC splits were assigned in these cases, based on the split for a single punch from that substrate. A brief description of the 5040 analysis, based on a thermal-optical technique (Birch and Cary, 1996), and its application to CNFs/CNTs (Birch, 2010) are provided as supplementary information (see Supplementary data, available at *Annals of Occupational Hygiene* online). Further details are provided elsewhere (Birch, 1998; Birch et al. 1999; Birch, 2002; Birch, 2003, 2004; Noll and Birch, 2008).

Metals

Filter samples were analyzed for metals by inductively coupled plasma with atomic emission spectroscopy (ICP-AES) (SpectroFlame EOP; Spectro Analytical Instruments Inc., Fitchburg, MA, USA) according to NIOSH 7300. Samples were analyzed for the following metals: Ag, Al, As, Ba, Be, Ca, Cd, Co, Cr, Cu, Fe, K, La, Li, Mg, Mn, Mo, Na, Ni, P, Pb, Sb, Se, Sr, Te, Ti, Tl, V, Y, Zn, and Zr. For comparison with the EC results for the 37-mm quartz-fiber filters, portions (usually two 1.5 cm^2 punches) were taken from the same filters and extracted overnight in a 3:1 nitric/perchloric acid mixture. The samples were then diluted to 12 ml and analyzed.

In addition to filter samples, three bulk samples of CNF materials produced during the survey were analyzed: one sample each from reactors A and B,

and the final product. Samples were placed into pre-weighed capped glass vials and weighed. They were then transferred to 125-ml beakers in a fume hood for digestion and analysis according to NIOSH Method 7300, modified for bulk carbon nanotubes. Specifically, for sample digestion, 4 ml of concentrated nitric acid and 11 ml of concentrated perchloric acid were added to each sample. The samples were covered with a watch glass and refluxed at 200°C until dissolution occurred. The watchglass covers were then removed and the samples were heated at 150°C until they had reached near dryness. The residues were dissolved in a dilute solution (4/1%) of nitric acid/perchloric acid (10 ml final volume) and analyzed for trace metals by ICP-AES.

RESULTS AND DISCUSSION

Specific surface area

The BET SSAs of the raw products were 2.0 m^2 g^{-1} for reactor A and 19.4 m^2 g^{-1} for reactor B, while that for the final product was 34.6 m^2 g^{-1}. The CNFs have outer diameters in the range of ~50 to 200 nm. Their surface areas are low relative to most CNTs, as expected based on the inverse relationship between diameter and SSA. Typical values for SWCNTs range from ~150 to 600 m^2 g^{-1} (Eswaramoorthy *et al.*, 1999; Fujiwara *et al.*, 2001; Cinke *et al.*, 2002; Martinez *et al.*, 2003; Kayiran *et al.*, 2004; Li *et al.*, 2004; Chakraborty *et al.*, 2006; Hemraj-Benny *et al.*, 2008) and from ~15 to 300 m^2 g^{-1} for MWCNTs (Tsang *et al.*, 1993; Yin *et al.*, 1999; Raymundo-Pinero *et al.*, 2002; Zhu *et al.*, 2003; Li *et al.*, 2004; Chen and Wang, 2006; Zacharia *et al.*, 2007; Naseh *et al.*, 2009).

Microscopy

Figure 1 shows TEM images of size-classified particles collected by Sioutas impactors located in the thermal treatment area. Most of the particles on the upper stages (A and B) were bundled/entangled structures. The fiber diameters in these structures range from ~60 to 250 nm, with lengths up to 4 μm. On the two lower stages (C and D), where the collected particle size decreases, particles were less entangled. There was no evidence of fibers on the after filter, indicating that most of the fibrous particles have aerodynamic diameters >0.25 μm. Nonfibrous soot-like particle clusters were present on all stages of the impactor, but they were mainly on the lower sections (Stages C and D), especially the after filter, which appeared yellowish. Particle number concentrations (Evans *et al.*, 2010) in this area showed a mode between 0.20 and 0.25 μm during a bag change, consistent with soot agglomerates observed by microscopy, while a second mode between 1 and 3 μm is consistent with the CNF structures. Based on particle number, CNFs represented just 0.035% of the particles in this area, precluding reliable measurement of their number-based concentrations and size distribution.

Figure 2a shows TEM images of particles collected by Sioutas impactors located in the reactor area. Particles on Stages A and B consisted of complex structures containing fibers and nonfibrous particulate matter and were similar to particles found in the thermal treatment area. Soot-like clusters (nonfibrous) having primary particles with diameters <30 nm were again found on Stages C and D, and nearly all of the particles on the after filter had this appearance. Also, the after filter again appeared yellowish. EDS analysis (Fig. 2b) of the after filter (cut point < 0.25 μm) indicated that these smallest clusters have high iron contents, up to 55% by weight. This result is consistent with the MOUDI substrates (Fig. 3) in that deposits on Stages 8 through 10 also were yellowish, with Stages 8 and 9 having a more intense color. Particles on these stages (8–10) have aerodynamic diameters <0.32 μm, the cut point of Stage 7, which is consistent with the size range (<0.25 μm) and color of the deposits on the final filters (not shown) of the Sioutas impactors. Some of these clustered particles also were present on Sioutas Stages C and D, which have cut points of 0.25 and 0.5 μm, respectively, but the vast majority were on the final filter. In addition to the carbon fiber bundles and soot-like clusters, fibers mixed with iron also were observed on Stage C.

An ESP sample (Fig. 4) collected in the reactor area shows a particle that appears to be an agglomerate of spherical primary particles with diameters ~200 nm. A particle of similar structure also is present in the material collected on Stage A of the Sioutas impactor (Fig. 2a). The EDS results for the ESP sample indicate carbon and iron as the major elements present.

In the maintenance area, where quality control (QC) samples were manually scooped into small zip-lock bags, fibers, and bundled structures again were observed (Fig. 5) on Stages A through D, but there were relatively few soot-like particles. Bagging was done on a bench located away from the reactor and thermal treatment areas, which may explain the relatively few soot-like particles present. The ESP results for samples collected in the dryer area of the facility contained a variety of particles of different shapes and sizes (Fig. 6),

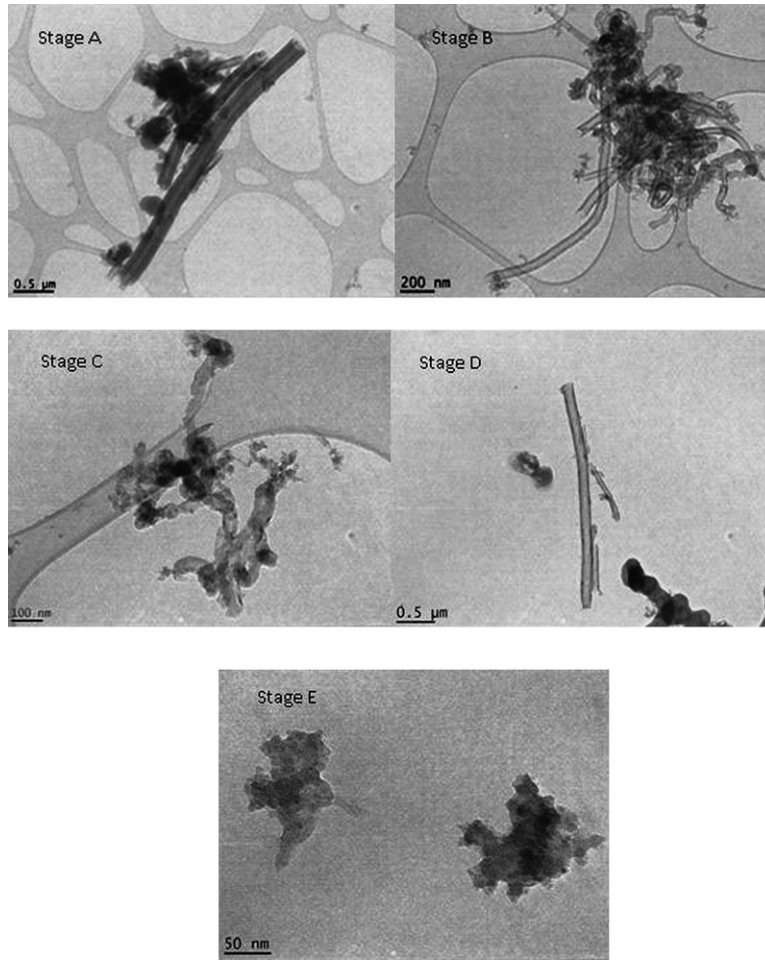

Fig. 1. Transmission electron microscopy images of particles size selected by impactors located in a thermal treatment processing area. Cut points are 2.5–10 µm (Stage A), 1.0–2.5 µm (Stage B), 0.5–1.0 µm (Stage C), 0.25–0.5 (Stage D), and <0.25 µm (Stage E after filter). Lacey carbon-coated Ni and SiO-coated Ni grids were used in impactors.

including fibers; however, soot-like particles were not found in these samples. Overall, particle morphologies were size dependent, with CNF-containing structures being mainly in the micrometer range. Iron-rich particles having a soot-like appearance with primary particle diameters of ~20 nm were dominant on Stages C, D, and the after filter of the Sioutas impactors. The particles on these lower two stages and after filter are similar, but those on the after filter have primary particles <20 nm that appear to be more fused together as aggregates than those on the upper stages.

Microscopy results for the bulk materials are shown in Fig. 7. A variety of structures were evidenced by TEM, including entangled fiber networks, isolated hollow tubes, and stacked-cup fibers (Fig. 7b–f,h,i). The SEM images (Fig.7a,g) show the overall form of the bulk materials, which consisted of relatively large clumps of highly entangled fiber networks. As expected, EDS analyses indicated iron in some of the sampled areas (spectra not shown).

OC and EC

OC and EC are useful air quality indicators, but EC was used as a measure of CNFs because they have negligible OC content and EC is a more selective marker. Figure 8 presents OC, EC, and TC (TC = OC + EC) results for total and respirable dust samples collected on two consecutive days in background locations (Fig. 8a) and in three processing/production areas, the thermal treatment area (Fig. 8b), and near the two reactors (Fig. 8c,d). Samples collected in the maintenance area (while a QC

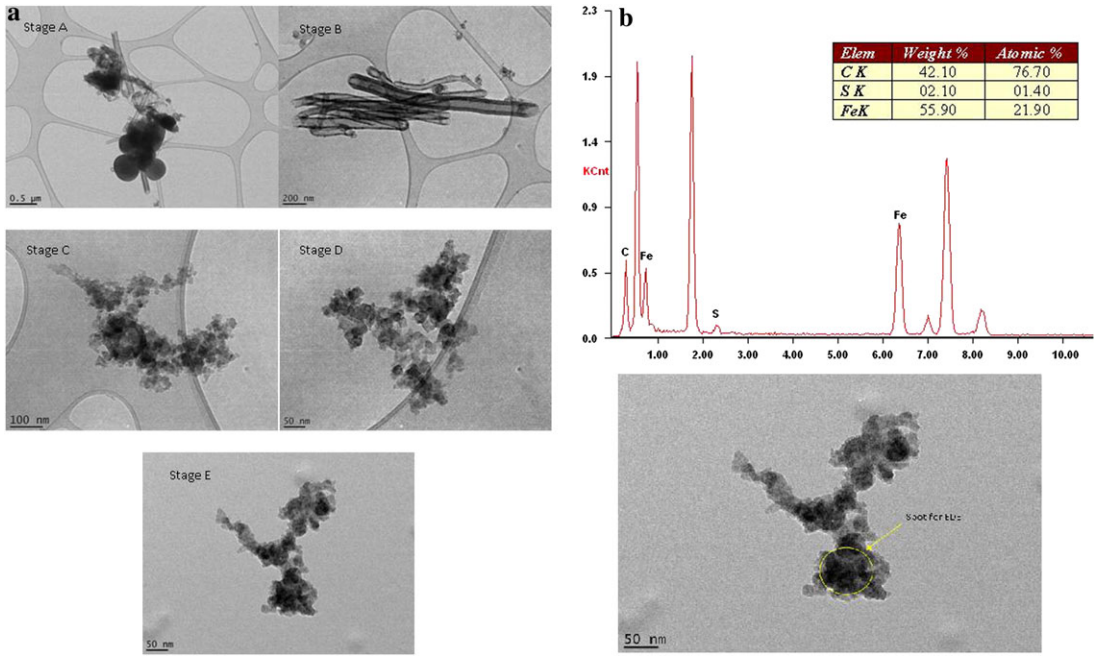

Fig. 2. (a) Transmission electron microscopy images of particles size selected by impactors located in the reactor area. Cut points are 2.5–10 µm (Stage A), 1.0–2.5 µm (Stage B), 0.5–1.0 µm (Stage C), 0.25–0.5 (Stage D), and <0.25 µm (Stage E after filter). Lacey carbon-coated Ni and SiO-coated Ni grids were used in impactors. (b) Energy-dispersive X-ray spectroscopy of portion of particle collected on Stage E (after filter) of impactor located in reactor area. SiO-coated Ni grid used. All particles on Stage E (<0.25 µm) were iron-rich (40–55% by weight).

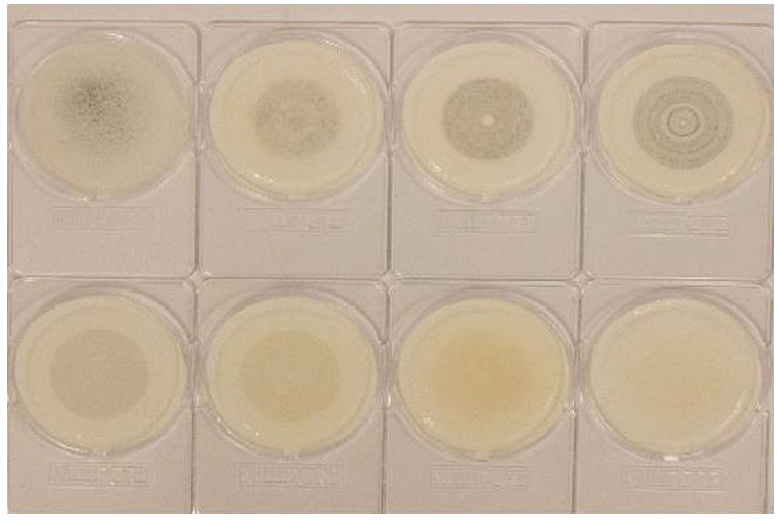

Fig. 3. MOUDI impactor substrates showing carbon nanofibers mainly on upper stages and iron aerosol on lower ones. Top row (left to right) shows Stages 0 (inlet), 2, 4, and 6. Bottom row (left to right) shows Stages 7 through 10.

sample was bagged) are not reported because the sampling period was too short (∼10 min) for reliable quantification. Results for two personal breathing zone samples of respirable dust collected on the second day in the thermal treatment (Fig. 8b) and reactor A (Fig. 8c) areas also are reported.

Respirable EC concentrations on the two consecutive sampling days ranged from 3.41 to ∼32 µg

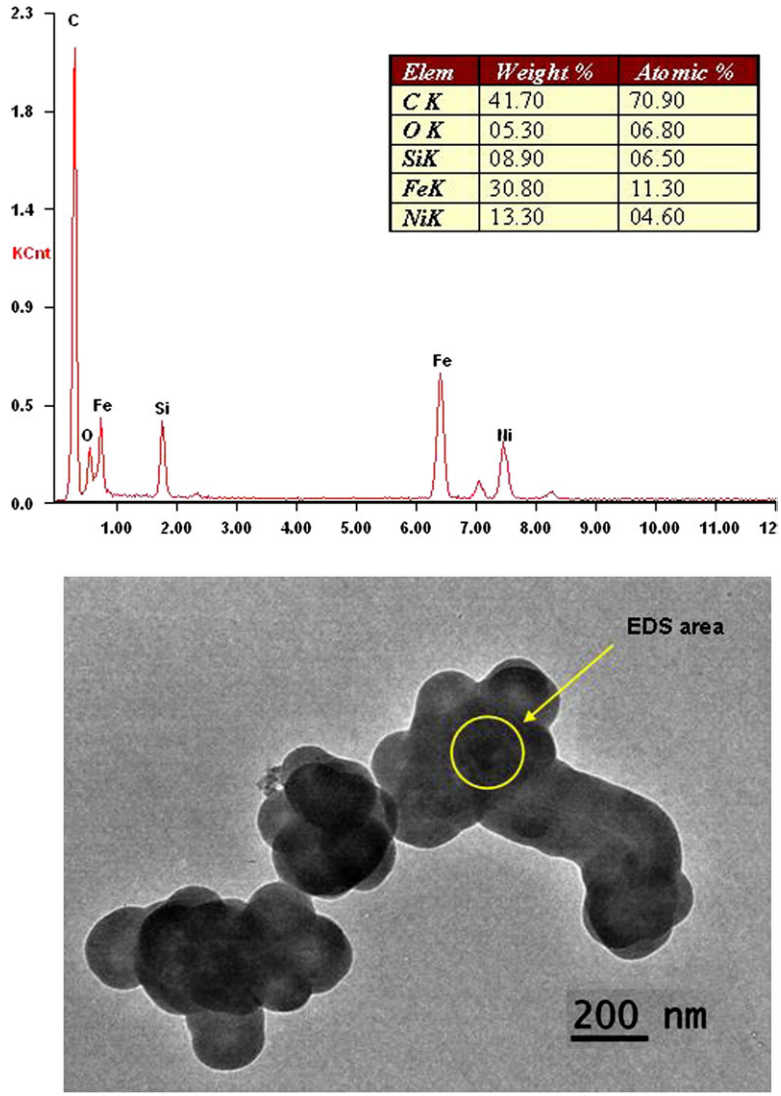

Fig. 4. Energy-dispersive X-ray spectroscopy of portion of particle sampled by electrostatic precipitator located in reactor area. SiO-coated Ni grid used. Area analyzed was ∼30% iron by weight.

m^{-3} in the process/production areas (Fig. 8b–d) [note: error bars in Figs 8–10 represent either the absolute difference between two results or the standard deviation (SD) for three or more (see Supplementary data, available at *Annals of Occupational Hygiene* online, for further details)]. Personal respirable EC results were higher than the corresponding area results. On Day 2, respirable EC for two employees working mainly in the thermal treatment and reactor A areas (Fig. 8b,c) were ∼45 and 80 μg m^{-3} (respectively), while the corresponding area samples were ∼32 and 13 μg m^{-3}. It is noteworthy that the EC concentration in the reactor A area was less than half that in the thermal treatment area, but the personal sample collected in this area (reactor A) was almost twice as high.

The respirable EC in the thermal treatment area (Fig. 8b) was lower on Day 1 of the survey, 3.41 μg m^{-3} as opposed to 31.80 μg m^{-3} on Day 2; however, this increase reflects a change in sampling location. Sampling locations on the 2 days were identical for the reactor area samples, but samplers in the thermal treatment area were moved closer to the product discharge point on Day 2 to check the CNF air

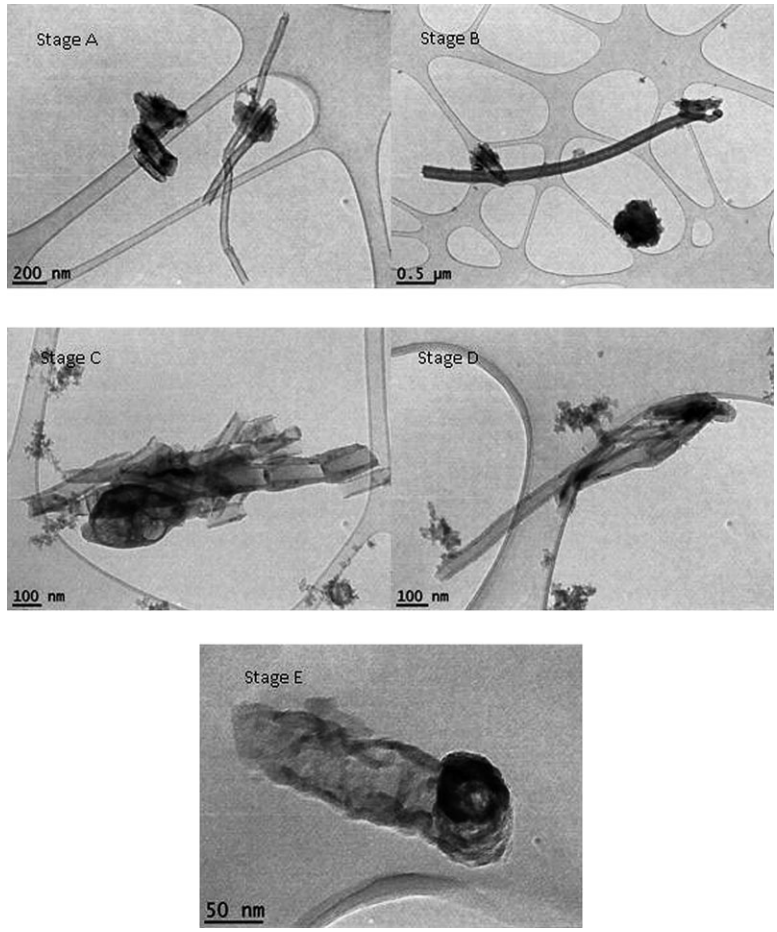

Fig. 5. Transmission electron microscopy images of particles size selected by impactors located in a bagging area. Cut points are 2.5–10 μm (Stage A), 1.0–2.5 μm (Stage B), 0.5–1.0 μm (Stage C), 0.25–0.5 (Stage D), and <0.25 μm (Stage E after filter). Lacey carbon-coated Ni and SiO-coated Ni grids were used in impactors.

concentration at this location. For this reason, the respirable EC concentration in the thermal treatment area was higher (by nine times) on Day 2.

The EC (and OC and TC) concentrations near reactor A (Fig. 8c) were higher than those near reactor B (Fig. 8d), likely due to differences in reactor design (B is newer), the form of the raw CNF materials discharged, and manual handling procedures. The respirable EC concentrations in these two areas were about the same on both days: 11.25 and 12.95 μg m^{-3} near reactor A, and 4.68 and 4.55 μg m^{-3} near reactor B.

Relative to the outdoor total EC, the EC concentrations found in the reactor A (Fig. 8c) area on the 2 days were 53 and 46 times higher for the total dust samples, while the two respirable dust samples were 24 and 28 times higher. Personal respirable EC concentrations for two employees working primarily in the thermal treatment and reactor A areas on Day 2 (Fig. 8b,c) were (respectively) 96 and 170 times higher than the total outdoor EC. Samples collected in an office area (Fig 8a) also showed elevated EC relative to outdoors. The total EC, at 8.07 μg m^{-3}, was ∼17 times higher in an office area than outdoors, and the respirable EC, at 1.53 μg m^{-3}, was 3.3 times higher. The much lower respirable relative to total EC in the office area indicates that larger non-respirable particles contributed to the total EC in this area. A probable contamination route is tracking of material on footwear from the process areas. The room, a conference room in the office area, was carpeted and material may have accumulated in the carpet. Foot traffic and ceiling-mounted heating/cooling vents in the room may have contributed to resuspension of CNF material.

Two additional surveys were conducted 2 months later, on 2 days (in February) 1 week apart. Results

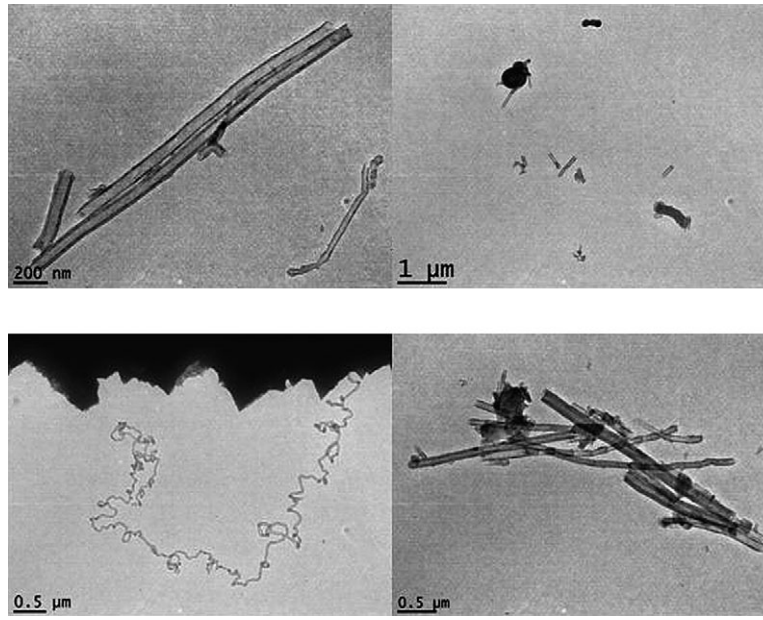

Fig. 6. Transmission electron microscopy images of polydisperse particles sampled by an electrostatic precipitator operated in the dryer area. SiO-coated Ni grid was used for sampling.

for these two survey days are shown in Figs 9 and 10. During these surveys, thoracic dust samples were collected in addition to total and respirable dust. Air samples also were collected in the control room of the facility. The total outdoor EC (Figs 9a and 10a) on the 2 days was 0.51 and 0.48 µg m^{-3}, nearly identical to the result (0.47 µg m^{-3}) obtained 2 months earlier. The total and respirable EC concentrations for samples collected in the reactor (Figs 9b and 10b) and thermal treatment areas (Figs 9c and 10c) also were comparable to those obtained previously, ranging from ~3 to 22 µg m^{-3}. For all indoor areas sampled, the highest EC concentrations were found with the total dust samplers, followed by thoracic and then respirable.

As found previously, personal breathing zone samples were higher than area samples. On the first sampling day, personal thoracic EC (35.10 µg m^{-3}) in the reactor A area (Fig. 9b) was ~69 times higher than outdoor total EC and 2.3 times higher than a thoracic sample taken in the same area. In the thermal treatment area (Fig. 9c), the personal thoracic EC (46.32 µg m^{-3}) was 90 times higher than the total outdoor EC and 9 times higher than a thoracic sample collected in this area. On the second survey day, EC concentrations for personal thoracic samples collected in the thermal treatment (Fig. 10c) and reactor A (Fig. 10b) areas (27.29 and 19.33 µg m^{-3}, respectively) were ~57 and 40 times higher than the total outdoor EC. The personal thoracic sample collected in the thermal treatment area on Day 2 (Fig. 10c) was 2.3 times higher than a 'total' (note: a thoracic area sample was not collected in the thermal treatment area on Day 2) EC area sample, while the personal thoracic EC sample collected in the reactor area (Fig. 10b) was 1.3 times higher than a thoracic sample from this area.

Results for the control room were significantly different on the two sampling days. The total EC on the first sampling day (Fig. 9d) was ~75 µg m^{-3}, while it was ~20 µg m^{-3} on the second day (not shown). This difference is attributed to operation of a wall air conditioner in the room on Day 1 but not on Day 2. The air conditioner was mounted in the wall ~3 feet from the floor and likely resuspended CNF contamination (e.g. tracked in by footwear) in the room; contamination was apparent on the floor and other surfaces. The respective thoracic and respirable EC concentrations (Fig. 9d) on Day 1 were ~43 and 24 µg m^{-3}. Thoracic and respirable EC concentrations in the control room on Day 2 are not reported because only total EC was collected that day.

Metals

As determined by EDS, iron was the dominant airborne metal found by ICP/AES. This was expected based on use of an iron-containing catalyst precursor in the CNF synthesis. Several other metals were

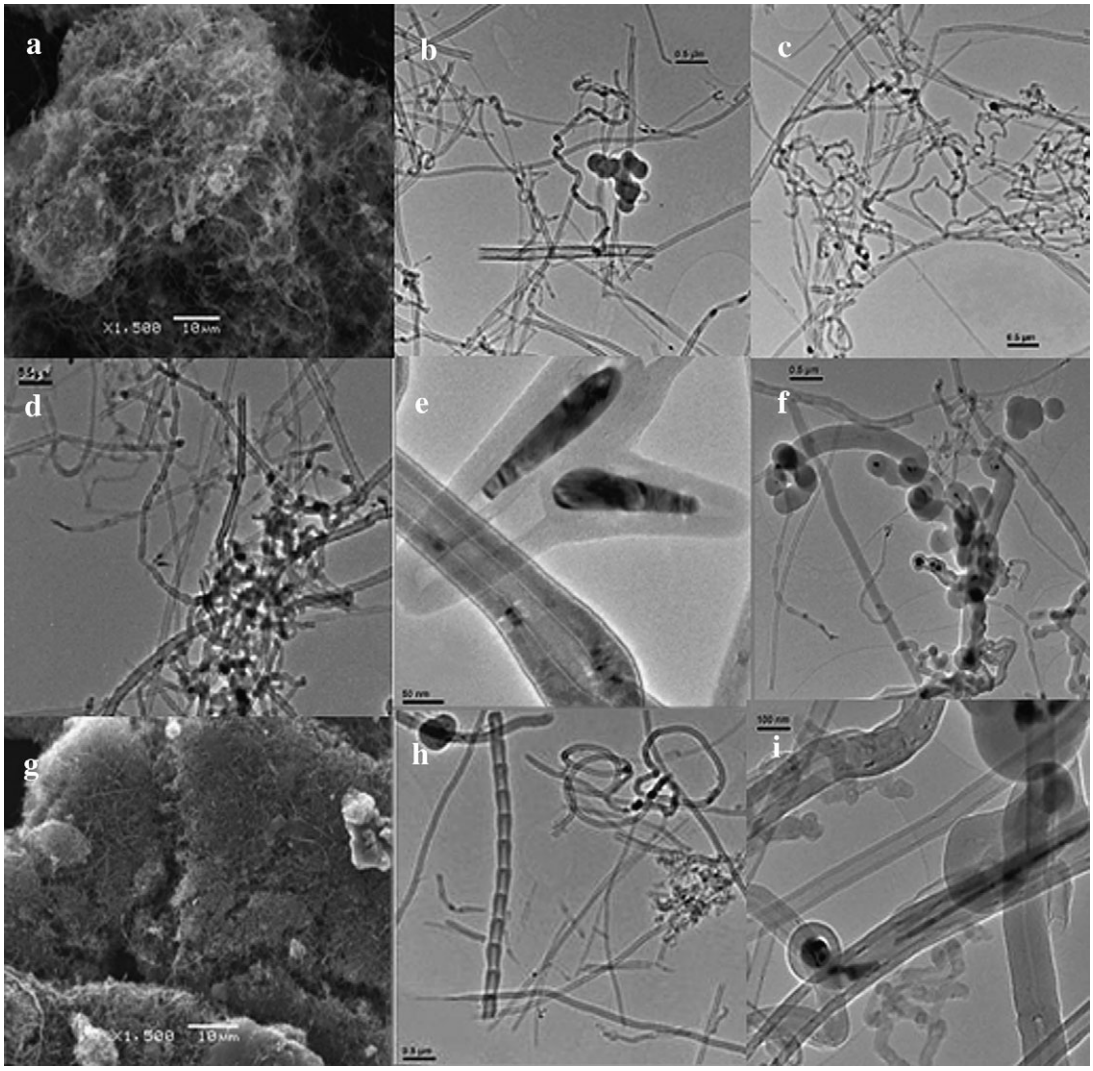

Fig. 7. Transmission electron microscopy (b–f, h, i) and scanning electron microscopy (a, g) images of bulk carbon nanofiber materials. Images (a–f) are unprocessed materials. Images (g–i) are processed product. Scale bars are: (a) and (g) = 10 μm; (b–d) and (h) = 500 nm; (e) = 50 nm; (f and i) = 100 nm.

found, but results are not reported because they are between the method limits of detection and quantitation (LOD and LOQ), with some results comparable to the blanks.

Air concentrations of iron and the corresponding EC concentrations found during the first 2 (consecutive) days of the survey are plotted in Fig. 11a. Unlike EC, the iron concentrations in the reactor (A and B) and plant background areas, as well as the personal sampler result for the reactor area, were quite similar over the 2 days. Also unlike EC, results for the total and respirable aerosol samples were equivalent. The mean iron concentration found with total and respirable aerosol samples collected over the 2 days in these areas was 9.87 μg m^{-3} [n = 9, relative standard deviation (RSD) = 14.73%]. If two area samples in the thermal treatment area are included, the mean iron concentration for the four locations was 10.31 μg m^{-3} (n = 11, RSD = 19.37%). The personal sample in the thermal treatment area was almost four times higher than the mean and was not used in its calculation. The personal sample may have been elevated relative to the area samples because the worker climbed stairs to load a hopper that feeds the thermal treatment system.

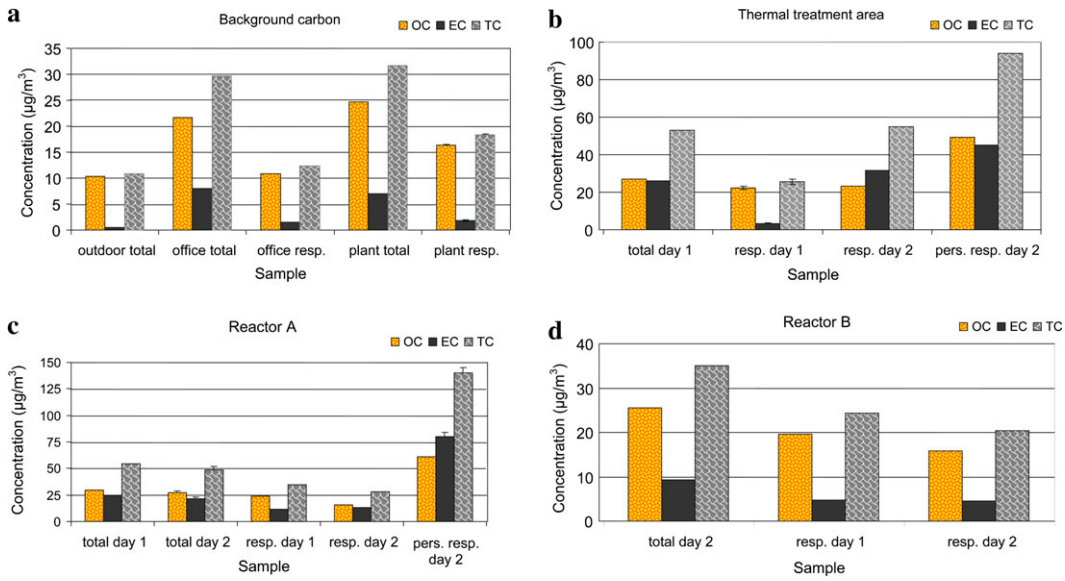

Fig. 8. (a) Average OC, EC and total carbon (TC) results for total and respirable (resp.) dust samples collected outdoors and in office and plant background areas of the facility on two consecutive days in December. (b) Average OC, EC, and TC results for total and resp. dust samples collected in the thermal treatment area of the facility on two consecutive days in December. (c) Average OC, EC, and TC results for total and resp. dust samples collected in the reactor A area of the facility on two consecutive days in December. (d) Average OC, EC, and TC results for total and resp. dust samples collected in the reactor B area of the facility on two consecutive days in December.

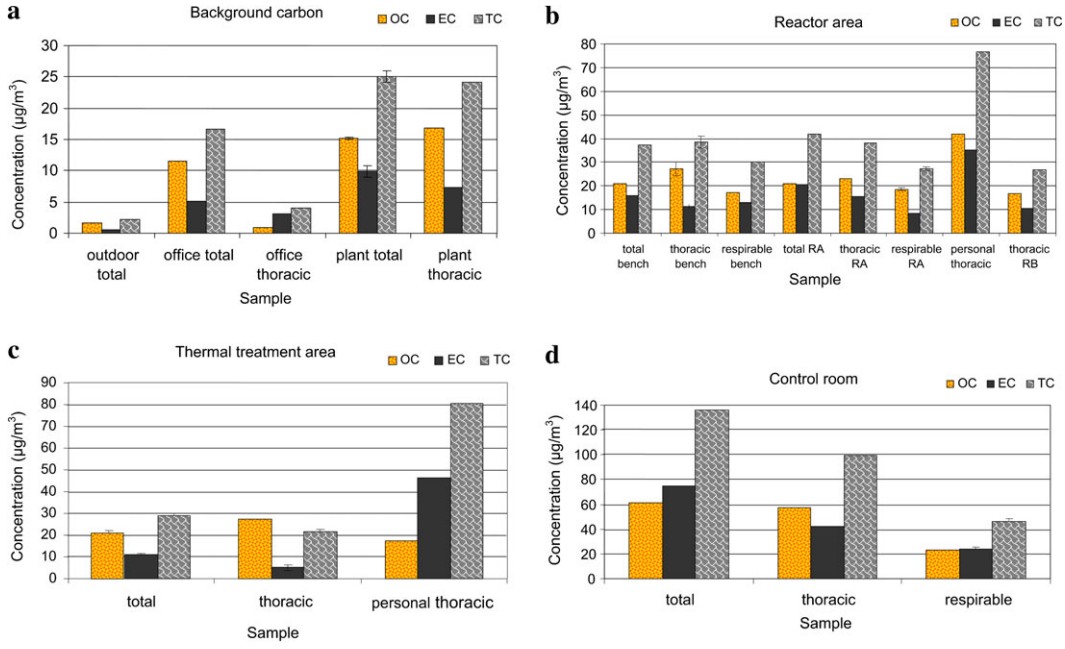

Fig. 9. (a) OC, EC, and TC results for total and thoracic dust samples collected outdoors and in office and plant background areas of the facility on the first survey day in February. (b) OC, EC, and TC results for total, thoracic, and respirable dust samplers located in the reactor area of the facility on the first survey day in February (RA and RB indicate reactors A and B). (c) OC, EC, and TC results for total and thoracic dust samplers located in the thermal treatment area of the facility on the first survey day in February. (d) OC, EC, and TC results for total, thoracic, and respirable dust samplers located in the control room of the facility on the first survey day in February.

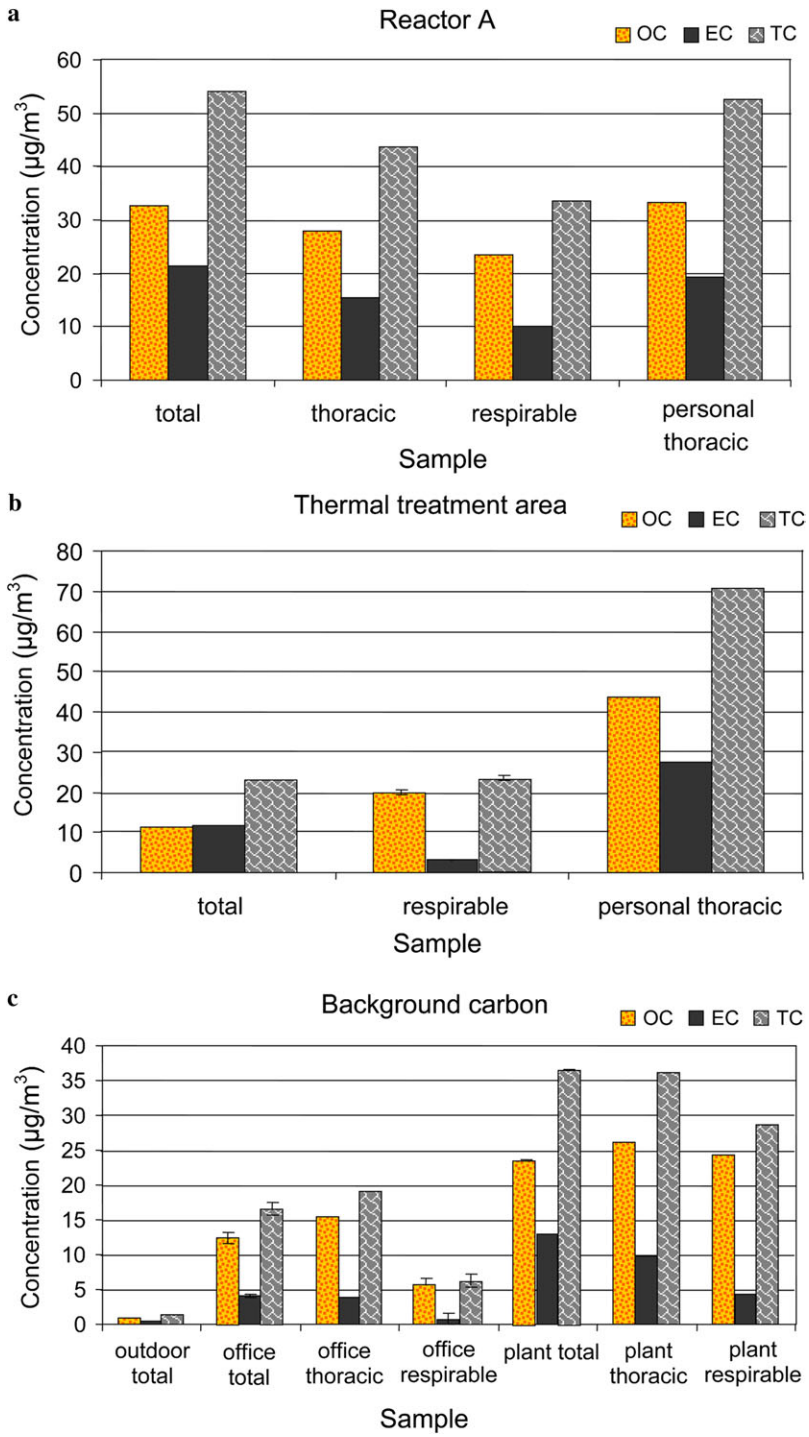

Fig. 10. (a) OC, EC, and TC results for total, thoracic, and respirable dust samples collected in the reactor A area of the facility on the second survey day in February. (b) OC, EC, TC results for total, thoracic, and respirable dust samples collected in the thermal treatment area of the facility on the second survey day in February. (c) OC, EC, and TC results for total, thoracic, and respirable dust samples collected outdoors and in office and plant background areas of the facility on the second survey day in February.

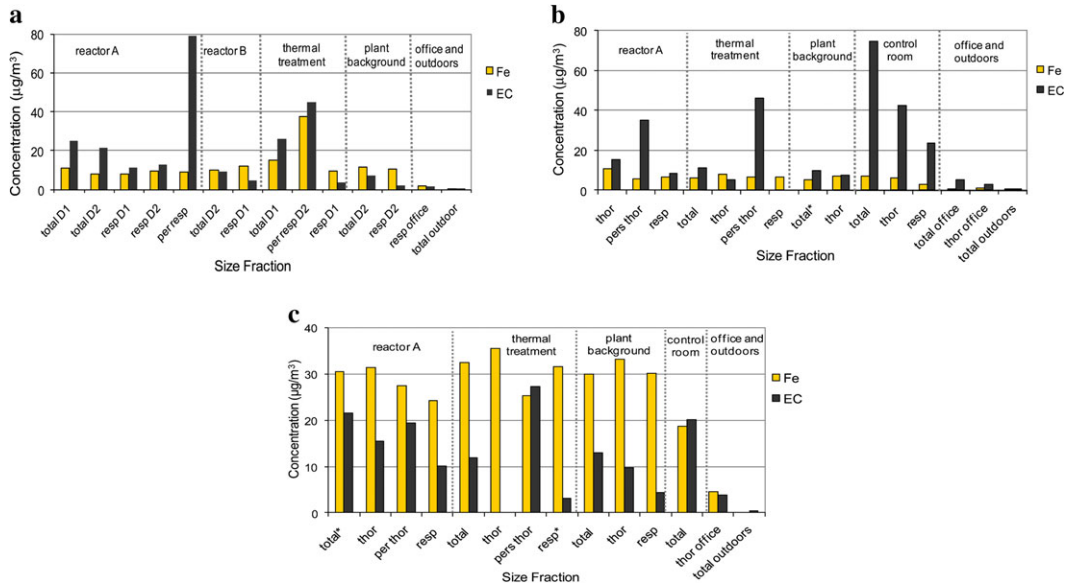

Fig. 11. (a) Total and respirable (resp.) iron (Fe) and EC concentrations in different areas of the facility and outdoors. 'Pers. resp.' is personal (breathing zone) respirable sample. Respirable plant background on Day 2 (resp. D2) is average for two samplers. Outdoor sample was nondetect. Surveys conducted on two consecutive days (D1 and D2) in December. (b) Total, thoracic (thor), and resp. Fe and EC concentrations in different areas of the facility and outdoors. Breathing zone thoracic sample. Asterisk indicates Fe result based on one filter punch; other Fe results based on two. Total Fe in thermal treatment area is average of one punch from two samplers; outdoor sample was nondetect. Survey conducted during first week of February. (c) Total, thor, and resp. iron Fe and EC concentrations in different areas of the facility and outdoors. Breathing zone thoracic sample. Asterisk indicates Fe result based on one filter punch; other Fe results based on two. Total Fe in thermal treatment area is average of one punch from two samplers; outdoor sample was nondetect. Survey conducted during second week of February.

Emissions from the system, upon opening the hopper, and possibly from the ductwork, may be responsible for the higher result.

Further air sampling was conducted on two additional days 2 months after the initial surveys. Results for these surveys are plotted in Fig. 11b,c. Results of the first survey (Fig. 11b), conducted during the first week of February, were similar to those found over 2 days 2 months earlier. Iron concentrations in the reactor (A), thermal treatment, and plant background areas averaged 7.09 µg m^{-3} (n = 9, RSD = 22%), and the personal samples (included in the mean) were equivalent to area samples. Unlike the result for the first survey, the personal sample collected in the thermal treatment area was comparable to the area samples, possibly because fewer trips to the hopper feeding the thermal treatment system were made. Though the iron concentration found for the personal sample collected in the thermal treatment area was more than five times higher during the previous survey, the personal EC concentration (45 µg m^{-3}) was almost identical to that (46 µg m^{-3}) found previously. Also of interest, iron concentrations were elevated (relative to outdoors) in the control room and in an office area, which are separated (by walls) from the main open-floor plant area.

Results of the second survey (in February), conducted 1 week after the first, are shown in Fig. 11c. Trends are similar to the earlier surveys, but the iron concentrations were much higher this day. The average iron concentration in the reactor (A), thermal treatment, and plant background areas, and for the personal samplers, was 30.14 µg m^{-3} (n = 11, RSD = 11.08%), which is about three times higher than previous results. Only the iron concentration was affected. The EC concentration range is consistent with results for previous surveys. Reactor maintenance this day may explain the increase.

In December, the personal sample iron result, 37.34 µg m^{-3}, for the thermal treatment area was almost four times higher than the area mean for iron, but this is not related to CNF exposure. The iron and EC results demonstrate that airborne CNFs were not a significant source of the iron aerosol found in this facility. For example, the EC result for a personal sample collected in the reactor area in December is nearly 80 µg m^{-3}, while the iron result (9.16 µg m^{-3}) is slightly below the mean (~10 µg m^{-3}). On

the other hand, the plant background EC was much lower, 1.87 μg m^{-3}, than the result for the personal sample, but the iron concentration was slightly above the mean. Iron emissions from the reactors are generated as a separate aerosol through decomposition of the catalyst precursor employed for CNF synthesis, explaining both the elevated CO (Evans *et al.*, 2010) and fine/ultrafine particle emissions. Thermal treatment of the raw material also generated iron-containing aerosol. As discussed earlier, iron-rich particles were evidenced by TEM/EDS analyses. Soot-like clusters with primary particle diameters <30 nm were found (on Sioutas impactor Stages C, D, and after filter), and EDS analysis (Fig. 2a) of particles on the after filter (<0.25 μm) of a Sioutas impactor indicated that these were up to 56% iron by weight. Also as mentioned, MOUDI substrates showed yellowish deposits on Stages 8 through 10 (Fig. 3). Particles on these stages have aerodynamic diameters <0.32 μm, consistent with the size range (<0.25 μm) and color of deposits on the final filters of the Sioutas impactors. Further discussion of the Sioutas and MOUDI results for iron and EC is provided in the next section.

Equivalence between the total and respirable aerosol results for both area and personal samples collected in the different areas indicates that the iron-containing aerosol is well mixed and fully respirable. Given the relatively low spatial variation in the fine/ultrafine iron aerosol concentration, the overhead ductwork that exhausts reactor byproducts and thermal treatment emissions may be the main source of this aerosol rather than ground-level sources.

Results for the bulk CNF materials also indicated iron as the dominant metal (attributed to the iron-containing catalyst precursor). As with the air samples, other trace metals were found but results are not reported because they fell between the LOD and LOQ and/or were near the blank values. Iron results (blank corrected) for the three samples were comparable. Mass percentages for raw products A and B, and the final product were 0.99, 0.98, and 1.07%.

Cascade impactor results: iron and EC

Iron and EC results for the Sioutas and MOUDI impactors are shown in Fig. 12a–c. Figure 12c presents combined results for Sioutas and MOUDI impactors located in the thermal treatment area on the initial survey day. The Sioutas results (four stages and after filter) are indicated by '(S)' after the particle size range. As explained earlier, EC results for the MOUDI are reported only for Stages 1, 3, and 5 because the lower stages could not accommodate the pressed quartz filters without excessive back pressure. Also, only Sioutas results are reported for the reactor (A) area because a problem was encountered with the MOUDI in this area and results were therefore voided.

In both the thermal treatment and reactor areas (Fig. 12a–c), iron was dominant in the size fraction <0.25 μm, while most of the EC was in the 2.5–10 μm range. Consistent with the results for the total and respirable samples, there is no correlation between the iron and EC concentrations, which is expected for reasons discussed in the preceding section (see Metals).

Health implications of mixed aerosol exposures

Exposure to fine/ultrafine iron particles alone may be inconsequential at the concentrations reported in this study, but exposure to iron, EC (in soot and CNFs), and PAHs may not be. EC particles in some mixtures may serve as potential reducing agents and thereby increase the biological response to inhaled particulate matter. Specifically, iron combined with soot can induce respiratory tract responses not caused by iron or soot alone. Inhalation exposure of young adult rats demonstrated a strong synergistic interaction between iron and soot particles (Zhou *et al.*, 2003). Animals exposed to a soot concentration of 250 μg m^{-3} showed no adverse respiratory effects. Similarly, no effects were found with exposure to iron aerosol at 57 μg m^{-3}. In contrast, addition of 45 μg m^{-3} of iron aerosol to soot aerosol, with a total mass concentration of 250 μg m^{-3}, resulted in significant pulmonary ferritin induction, oxidative stress, and elevation of proinflammatory pulmonary cytokines. *In vitro* studies also suggest synergistic effects between iron and EC particles. Co-exposure of human lung epithelial cells (A549) to carbon black and iron oxide (Fe_2O_3) nanoparticles caused a synergistic oxidative effect that was significantly greater than the additive effects of exposures to either particle type alone (Guo *et al.*, 2009).

The combined iron–CNF (as EC) exposures found in our study were <250 μg m^{-3}, but the pulmonary toxicity of the iron–CNF aerosol may be greater than that for iron and soot because of the CNF structure and PAH content. The combined iron and EC concentrations for personal samples over different survey days were ~89, 82, 41, 53, 47, and 53 μg m^{-3}. The corresponding iron-to-EC mass fractions for these samples were 0.12, 0.83, 0.16, 0.15, 1.42, and 0.93, respectively, while the iron-to-soot ratio in the animal study (Zhou *et al.*, 2003) was ~0.22. The potential influence of the proportions of iron and soot on aerosol toxicity was not examined.

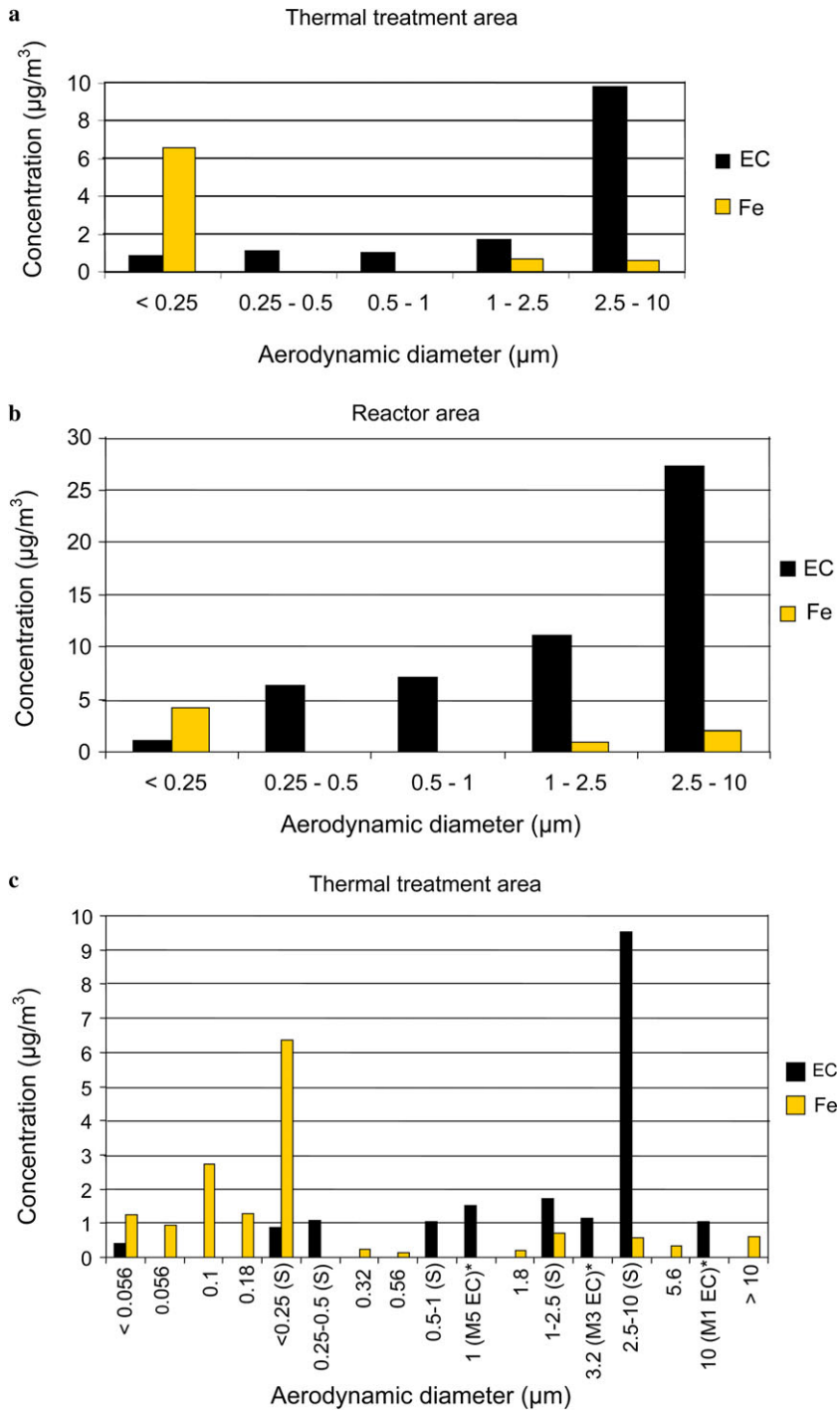

Fig. 12. (a) Iron (Fe) and EC results for impactors in the thermal treatment area on the initial survey day. (b) Fe and EC results for impactors in the reactor area on the initial survey day. (c) Fe and EC results for Sioutas and MOUDI impactors located in the thermal treatment area on the initial survey day. Sioutas results are indicated by '(S)' after the particle size bin. MOUDI EC results are reported for Stages 1, 3, and 5 only (see text). Asterisk indicates Fe result based on one filter punch; all other Fe results based on two.

Exposure metrics

Several studies indicate that the inhalation toxicity of some materials is greater for particles in the fine (<2.5 μm) and ultrafine (<100nm) range than for larger particles of the same material (Oberdorster *et al.*, 1995; Johnston *et al.*, 2000; Karlsson *et al.*, 2009). Based on these findings, surface area was suggested as a more relevant exposure metric for nanoscale aerosols than mass (Maynard and Maynard, 2002; Moshammer and Neuberger, 2003). If the biological response to inhaled fine/ultrafine insoluble particles with roughly spherical dimensions is due mainly to interactions with surface species (e.g. metals, functional groups, adsorbed species), these findings might be expected given the high surface area of particles in this size range. However, for CNF/CNT aerosols, factors such as particle structure (agglomerates versus discrete fibers), aerodynamic behavior, durability, and metal content may be better determinants of potential health effects than surface area. Though SSA can provide insight on the properties of CNF/CNT materials, measurement in the field is not practical, and the BET analysis requires tens of milligrams of material. A portable direct-reading instrument that measures 'active' surface area was applied in our study (Evans *et al.*, 2010), but it was not a useful indicator of CNFs. Further, the relationship between the SSA of a bulk powder and active surface area of an aerosol is not well defined.

In our study, EC was a quantitative measure of CNFs, while other metrics (e.g. SSA, metals, PAHs, microscopy) were useful in characterizing the CNF materials and in characterizing/quantifying other emissions. As reported in our previous paper on the direct-reading monitoring results of this study, respirable mass estimated by a photometer was the most useful on-site indicator of CNFs (Evans *et al.*, 2010). Total particle number (9.0×10^4 to 1.15×10^6 cm^{-3}) and active surface area (430–1440 μm^2 cm^{-3}) concentrations, as monitored by a condensation particle counter and diffusion charging-based instrument, were not useful indicators of CNFs. Fine/ultrafine particles dominate the responses of these instruments. In this facility, they provided a relative measure of byproduct emissions (e.g. iron-EC soot and particles with condensed PAH) rather than CNFs. In contrast, most of the EC mass was contributed by particles in the 2.5–10 μm size fraction, indicating that CNFs were the dominant EC source. Similar findings for CNTs were reported in a previous study (Maynard *et al.*, 2004), wherein particle number and CNT mass were poorly correlated and increases in fine/ultrafine particles were attributed to operation of a vacuum cleaner.

Transient increases in mass concentration were observed with the photometer when the CNF material was handled manually (Evans *et al.*, 2010). Airborne CNFs also were visible, indicating agglomerated material, and relatively large fiber bundles were evidenced by microscopy. Observation of the CNF processing steps and photometer readings indicated that exposure occurs mainly during material handling. Thus, short-term transient exposures were much higher than reflected by the time-integrated EC results for samples collected over several hours. Based on photometer readings, transient exposures to CNFs may have exceeded 1 mg m^{-3} during manual handling. Short-term (e.g. 10 min) filter samples were collected during bagging of a QC sample, but the CNF mass was insufficient for quantification. Alternative procedures (e.g. higher flow rates and 25-mm filters) can be applied to improve the method detection limit (Birch, 2010).

As discussed (see Metals), iron was not a useful indicator of CNF exposure in this facility. Because the major iron source was not CNF derived, there was no correlation between the iron and CNF concentrations. Even if iron (or another metal) was a selective marker of CNF exposure, the LOD for ICP/AES analysis is not low enough to use iron as a surrogate measure of CNFs at low concentrations (e.g. near the EC LOQ). The iron LOD and LOQ were 0.12 and 0.4 μg iron/sample, respectively. If the SD for the EC results for media blanks is taken as 0.03 μg EC per cm^2 (a typical value), the filter mass loading corresponding to the EC LOQ would be ~0.30 μg EC per cm^2. At only 1% iron, the corresponding iron loading would be ~0.003 μg iron per cm^2. Thus, even if two 1.5-cm^2 filter punches are analyzed, as was done with most samples in this study, the total iron mass (~0.01 μg) at the EC LOQ would be well below the ICP/AES LOQ for iron (and also below the reported LOD for samples in this study). Methods such as ICP/MS offer detection limits superior to ICP/AES, but minimal background interference and correlation with CNF/CNT mass (or other relevant metric) would be required if a metal is used as an exposure metric.

CONCLUSIONS

Filter, sorbent (for PAHs), impactor, microscopy, and bulk samples, combined with direct-reading instruments, provided complementary information on air contaminants generated during the manufacture and processing of CNFs. Exposure was to

a complex mixture of CNFs, fine/ultrafine iron-rich soot, PAHs (Birch, 2011), and CO (Evans *et al.*, 2010). EC was a quantitative measure of CNFs, but iron (catalyst) was not a useful marker as CNFs were a negligible source. At metal contents of $\leq$1%, metal markers of CNFs/CNTs may be below the detection limits of commonly used methods, particularly at low air concentrations. Further, if a metal is used as an exposure index, minimal background and correlation with CNF/CNT mass or other relevant metric are required.

Because area samples are often not predictive of personal exposure, in this study not even in a relative sense, extrapolating personal exposure from area concentrations should not be done without a thorough assessment of the workplace to establish whether a valid extrapolation is possible. Results for personal breathing zone samples were significantly greater than the corresponding area samples, mainly due to manual handling of CNF materials in open areas. Differences can be substantial, depending on the area sampled and the manner and frequency of manual handling. Also, short-term exposures during manual handling were much higher than reflected by the time-integrated EC results for samples collected over several hours. Of the direct-reading instruments, a photometer was useful in identifying CNF releases and estimating mass concentrations on site (Evans *et al.*, 2010). Instruments that measure particle number and surface area were indicators of byproduct emissions. Though not useful for monitoring CNFs, especially when background concentrations of fine/ultrafine particles are high and variable, these instruments can be useful indicators of overall air quality.

Carbon nanomaterials vary widely in their properties. Their properties must be characterized to better understand the dispersibility (air and lung), respirability, and toxicity of these materials, and to guide safe development and use. In the workplace, raw and purified products, byproducts, and other emissions should be considered when assessing exposure risks as the potential health effects may be additive or synergistic with co-exposures. The presence of PAHs (Birch, 2011) in unpurified CNFs is a health concern. Also of significance is the finding of iron-rich soot aerosol. Some studies indicate that EC and iron particles together produce oxidative effects much greater than either particle type alone. Systematic studies of such complex mixtures are needed to better understand how interactions between components may influence aerosol toxicity. Inhalation of CNFs/CNTs is the primary health concern and was the focus of this study, but dermal contact and ingestion are potential exposure routes that merit future investigation. Given the inhalation risks suggested by animal studies, efforts to reduce and control exposure to CNFs/CNTs are prudent.

SUPPLEMENTARY DATA

Supplementary data can be found at http://annhyg.oxfordjournals.org/.

Acknowledgements—The authors wish to acknowledge Donnie Booher, Dan Farwick, and Karl Feldman for assistance with air sampling equipment, and Greg Deye and Prasoon Diwakar for manuscript review. They also gratefully acknowledge the management and staff of the facility surveyed for their full support and cooperation.

Disclaimer—Findings and conclusions in this report are those of the authors and do not necessarily represent the views of the National Institute for Occupational Safety and Health. Mention of product or company name does not constitute endorsement by the Centers for Disease Control and Prevention.

REFERENCES

Baron PA, Deye GJ, Chen BT *et al.* (2008) Aerosolization of single-walled carbon nanotubes for an inhalation study. Inhal Toxicol; 8: 751–60.

BCC Research. (2010) Nanotechnology: a realistic market assessment. report code: NANO31D, Analyst: Andrew McWilliams; July 2010. Available at http://www.bccresearch.com/report/NAN031D.html. Accessed 12 December 2010.

Birch ME. (1998) Analysis of carbonaceous aerosols—interlaboratory comparison. Analyst; 123: 851–7.

Birch ME. (2002) Occupational monitoring of particulate diesel exhaust by NIOSH Method 5040. Appl Occup Environ Hyg; 17: 400–5.

Birch ME. (2003) Standard test method for monitoring diesel particulate exhaust in the workplace, published by ASTM as standard test method D 6877—03. West Conshohocken, PA: ASTM International.

Birch ME. (2004) Monitoring diesel particulate exhaust in the workplace. Chapter Q, NIOSH Manual of Analytical Methods (NMAM). In: Schlecht PC and O'Connor PF, editors. Third supplement to NMAM. 4th edn. Cincinnati, OH: Department of Health and Human Services, Public Health Service, Center for Disease Control and Prevention, National Institute for Occupational Safety and Health DHHS (NIOSH) Publication No. 2003–154. issue date 2003, published 2004.

Birch ME. (2010) Appendix C: NIOSH Method 5040. NIOSH current intelligence bulletin: occupational exposure to carbon nanotubes and nanofibers, NIOSH Docket Number: NIOSH 161-A. Available at www.cdc.gov/niosh/docket/review/docket161A/. Accessed 12 December 2010.

Birch ME. (2011) Exposure and Emissions Monitoring during Carbon Nanofiber Production—Part II: Polycyclic Aromatic Hydrocarbons. Ann. Occup. Hyg; 55: 1037–47.

Birch ME, Cary RA. (1996) Elemental carbon-based method for monitoring occupational exposures to particulate diesel exhaust. Aeros Sci Technol; 25: 221–41.

Birch ME, Dahmann D, Hennig-Fricke H. (1999) Comparison of two carbon analysis methods for monitoring diesel particulate levels in mines. J Environ Monit; 1: 541.

Chakraborty S, Chattopadhyay J, Peng H *et al*. (2006) Surface area measurement of functionalized single-walled carbon nanotubes. J Phys Chem B; 110: 24812–5.

Chen C, Wang X. (2006) Adsorption of Ni(II) from aqueous solution using oxidized multiwall carbon nanotubes. Ind Eng Chem Res; 45: 9144–9.

Cientifica. (2005) Market research report: carbon nanotubes global production. Available at http://www.mindbranch.com/listing/product/R386-42.html. Accessed 12 December 2010.

Cinke M, Li J, Chen B, Cassell A *et al*. (2002) Pore structure of raw and purified HiPco single-walled carbon nanotubes. Chem Phys Lett; 365: 69–74.

Eswaramoorthy M, Sen R, Rao C. (1999) A study of micropores in single-walled carbon nanotubes by the adsorption of gases and vapors. Chem Phys Lett; 304: 207–10.

Evans DE, Ku BK, Birch ME *et al*. (2010) Aerosol monitoring during carbon nanofiber production: mobile direct-reading sampling. Ann Occup Hyg; 54: 514–31.

Fujiwara A, Ishii K, Suematsu H *et al*. (2001) Gas adsorption in the inside and outside of single-walled carbon nanotubes. Chem Phys Lett; 336: 205–11.

Guo B, Zebda R, Drake SJ *et al*. (2009) Synergistic effect of co-exposure to carbon black and Fe_2O_3 nanoparticles on oxidative stress in cultured lung epithelial cells. Part Fibre Toxicol; 6: 4.

Hemraj-Benny T, Bandosz T, Wong S. (2008) Effect of ozonolysis on the pore structure, surface chemistry, and bundling of single-walled carbon nanotubes. J Colloid Interface Sci; 317: 375–82.

Holman MN. (2007) The nanotech report. 5th edn. New York, NY: Lux Research.

ISO/TS 27687:2008. (2008) Nanotechnologies: terminology and definitions for nano-object; nanoparticle, nanofibre and nanoplate. Geneva, Switzerland: International Standard Organization.

Johnston CJ, Finkelstein JN, Mercer P *et al*. (2000) Pulmonary effects induced by ultrafine PTFE particles. Toxicol Appl Pharmacol; 168: 208–15.

Karlsson HL, Gustafsson J, Cronholm P *et al*. (2009) Size-dependent toxicity of metal oxide particles—A comparison between nano-and micrometer size. Toxicol Lett; 188: 112–8.

Kayiran S, Lamari F, Levesque D. (2004) Adsorption properties and structural characterization of activated carbons and nanocarbons. J Phys Chem B; 108: 15211–5.

Kisin ER, Murray AR, Sargent L *et al*. (2010) Pulmonary response, oxidative stress and genotoxicity induced by carbon nanofibers. Toxicologist; 114: 169.

Ku BK, Emery MS, Maynard AD *et al*. (2006) In situ structure characterization of airborne carbon nanofibers by a tandem mobility-mass analysis. Nanotechnology; 17: 3613–21.

Ku BK, Maynard AD. (2005) Comparing aerosol surface-area measurements of monodisperse ultrafine silver agglomerates by mobility analysis, transmission electron microscopy and diffusion charging. J Aerosol Sci; 36: 1108–24.

Lee BG, Lee JH, Yang JS *et al*. (2010) Exposure assessment of carbon nanotube manufacturing workplaces. Inhal Toxicol; 22: 369–81.

Li F, Wang Y, Wang D *et al*. (2004) Characterization of single-wall carbon nanotubes by N_2 adsorption. Carbon; 42: 2375–83.

Lux Research. (2008) Nanomaterials state of the market Q3 2008: stealth success, broad impact. Boston, MA Available at http://www.luxresearchinc.com/. Accessed 12 December 2010.

Martinez M, Callejas M, Benito A *et al*. (2003) Sensitivity of single wall carbon nanotubes to oxidative processing: structural modification, intercalation and functionalization. Carbon; 41: 2247–56.

Maynard AD, Maynard RL. (2002) A derived association between ambient aerosol surface area and excess mortality using historic time series data. Atmos Environ; 36: 5561–7.

Maynard AD, Baron PA, Foley M *et al*. (2004) Exposure to carbon nanotube material: aerosol release during the handling of unrefined single-walled carbon nanotube material. J Toxicol Environ Health A; 67: 87–107.

Maynard AD, Ku BK, Emery M *et al*. (2007) Measuring particle size-dependent physicochemical structure in airborne single walled carbon nanotube agglomerates. J Nanopart Res; 9: 85–92.

Methner MM, Birch ME, Evans DE *et al*. (2007) Case study: identification and characterization of potential sources of worker exposure to carbon nanofibers during polymer composite laboratory operations. J Occup Environ Hyg; 4: D125–30.

Moshammer H, Neuberger M. (2003) The active surface of suspended particles as a predictor of lung function and pulmonary symptoms in austrian school children. Atmos Environ; 37: 1737–44.

Murray AR, Kisin E, Leonard SS *et al*. (2009) Oxidative stress and inflammatory response in dermal toxicity of single-walled carbon nanotubes. Toxicology; 257: 161–71.

Naseh M, Khodadadi A, Mortazavi Y *et al*. (2009) Functionalization of carbon nanotubes using nitric acid oxidation and DBD plasma. Proc World Acad Sci Eng Technol; 37: 177–9.

NIOSH. (2010) NIOSH current intelligence bulletin: occupational exposure to carbon nanotubes and nanofibers, NIOSH Docket Number: NIOSH 161-A. Available at www.cdc.gov/niosh/docket/review/docket161A/. Accessed 12 December 2010.

NIOSH. (2003) Diesel particulate matter (as elemental carbon). Method 5040 supplement (issue 3 date 3/15/03; published 2004). In NIOSH Manual of Analytical Methods. 4th edn. Cincinnati, OH: U.S. Department of Health and Human Services.Public Health Service, Centers for Disease Control and Prevention, National Institute for Occupational Safety and Health, DHHS (NIOSH) Publication; pp. 94–113.

Noll JD, Birch ME. (2008) Effects of sampling artifacts on occupational samples of diesel particulate matter. Environ Sci Technol; 42: 5223–8.

Oberdorster G, Celein RM, Ferin J *et al*. (1995) Association of particulate air pollution and acute mortality: involvement of ultrafine particles? Inhal Toxicol; 7: 111–24.

Poland CA, Duffin R, Kinloch I *et al*. (2008) Carbon nanotubes introduced into the abdominal cavity of mice show asbestos-like pathogenicity in a pilot study. Nat Nanotechnol; 3: 423–8.

Raymundo-Pinero E, Cazorla-Amoros D, Linares-Solano A *et al*. (2002) High surface area carbon nanotubes prepared by chemical activation. Carbon; 40: 1597–617.

Roco MC, Bainbridge WS. (2005) Societal implications of nanoscience and nanotechnology: maximizing human benefits. J Nanopart Res; 7: 1–13.

Shvedova AA, Kisin ER, Mercer R *et al*. (2005) Unusual inflammatory and fibrogenic pulmonary responses to single-walled carbon nanotubes in mice. Am J Physiol Lung Cell Mol Physiol; 289: 698–708.

Shvedova AA, Kisin E, Murray AR *et al*. (2008) Inhalation versus aspiration of single-walled carbon nanotubes in C57bl/6mice: inflammation, fibrosis, oxidative stress and mutagenesis. Am J Physiol Lung Cell Mol Physiol; 295: L552–65.

Tsang S, Harris P, Green M. (1993) Thinning and opening of carbon nanotubes by oxidation using carbon dioxide. Nature; 362: 520–3.

Wang H, Xu Z, Eres G. (2006) Order in vertically aligned carbon nanotube arrays. Appl Phys Lett; 88: 213111.

Wang H, Feng J, Hu X *et al*. (2007) Synthesis of aligned carbon nanotubes on double-sided metallic substrate by chemical vapor deposition. J Phys Chem C; 111: 12617–24.

Yamashita K, Yoshioka Y, Higashisaka K *et al*. (2010) Carbon nanotubes elicit DNA damage and inflammatory response relative to their size and shape. Inflammation; 33: 276–80.

Yin Y, Mays T, McEnaney B. (1999) Adsorption of nitrogen in carbon nanotube arrays. Langmuir; 15: 8714–8.

WTEC. (2007) WTEC panel report on international assessment of research and development of carbon nanotube manufacturing and applications. Available at http://www.wtec.org/cnm/CNM_final_report.pdf. Accessed 12 December 2010.

Zacharia R, Kim K, Hwang S *et al*. (2007) Intrinsic linear scaling of hydrogen storage capacity of carbon nanotubes with the specific surface area. Catalysis Today; 120: 426–31.

Zhou YM, Zhong ZY, Kennedy IM *et al*. (2003) Oxidative stress and NFkappaB activation in the lungs of rats: a synergistic interaction between soot and iron particles. Toxicol Appl Pharmacol; 190: 157–69.

Zhu W, Miser D, Chan W *et al*. (2003) Characterization of multiwalled carbon nanotubes prepared by carbon arc cathode deposit. Mat Chem Phys; 82: 638–47.